DEVELOPMENT OF A WAVELET-ASSISTED EDGE-DETECTION ALGORITHM FOR ASSESSING THE SIZE OF BREAST LESIONS ON US.

Hikimtzis Chrysovaladis. [*], **Sidiropoulos Konstantinos** [*], **Athanasiadis Emmanouil** [*], **Georgiou Harris** [**], **Dimitropoulos Nikos** [***] **and Cavouras Dionisis** [*]

[*] Medical Image and Signal Processing Laboratory, Department of Medical Instruments Technology, Technological Educational Institute of Athens.

[**] Univ. of Athens, Informatics & Telecommunications Dept., TYPA buildings, Univ. Campus, 15771, Athens, Greece.

[***] Medical Imaging Department, EUROMEDICA Medical Centre, 2 Mesogeion Avenue, Athens, Greece

e-mail: cavouras@teiath.gr, web page: http://medisp.bme.teiath.gr

One hundred and fifty US mammograms were processed using an edge detection algorithm, developed in C++. A uniform histogram equalization filter was first applied, followed by a wavelet-based soft thresholding algorithm for speckle-noise suppression. A Laplacian mask and a Morphologic filter, involving binary dilation, were then applied for enhancing image edges and filling image holes respectively. Next, an active contour segmentation algorithm was applied for delineating the boundaries of target objects such as cysts, tumors etc. Finally, an area-filling algorithm was employed to calculate the total number of pixels within each lesion. The results were statistically compared with the free-hand target-object outline drawn by the physician (N.D.).

Agreement between areas selected by the physician versus areas calculated by the proposed algorithm was 92%. Overall processing time was less than 3s, requiring only minimum operator intervention

1.Introduction

A combination of image processing algorithms [1-3] was used to separate objects from the entire image for further observation and identification. The final purpose of the algorithm was to extract the target object from the image, define the edges' coordinates and measure the surface of the object in pixels. Moreover, a percentage difference in the region-of-interest (ROI) surface between the manually selected area and the automatically identified object boundaries, was calculated by the algorithm. The manual selection was conducted by an expert physician (D.N.), employing subjective positioning of a set of 12-15 reference points around the boundaries of the target object. The computation involved edge-detection processing, combined with global image thresholding and application of dynamic spline contour model ("snake") on the binary image. Images were pre-processed by a histogram equalization technique and a 3-level wavelet soft-thresholding algorithm[3].

2.Methods and Materials

One hundred and fifty US mammographic images with lesions (7 simple cysts, 32 complicated cysts, 52 malignant and 59 benign solid masses) were captured by means of a HDI-3000 ATL digital ultrasound system with a wide band (5-12 MHz) probe. Images were digitized by connecting the video output of the ultrasound scanner to a Screen Machine II frame grabber with 512x521x8 image resolution. US images are degraded by speckle noise that renders the application of automatic edge detection operators difficult. The convolution of a 3x3 median mask can effectively remove speckle noise with limited blurring of the object boundaries [3], as well as it can smooth the gray level transitions within homogeneous areas, thus improving the subsequent application of histogram thresholding and edge detectors. The 3-level wavelet soft thresholding (SWTF) was also employed for noise suppression. The wavelet coefficients of the first decomposition level were modified according to equation (1) as shown in Figure 1. The absolute values of the detail wavelet coefficients smaller than the threshold T were set to zero. Detail values higher than the threshold T were substituted by the same value minus T, while detail values lower than –T were substituted by the same value plus T.

$$W_{out}(W_{in}) = \begin{cases} 0 & \text{if } |W_{in}| \le T \\ W_{in} - T & \text{if } W_{in} > T \\ W_{in} + T & \text{if } W_{in} < -T \end{cases} \qquad \text{Eq(1).}$$

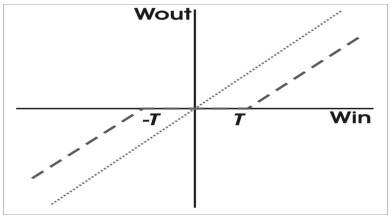

Figure 1: Soft wavelet thresholding (SWTF)

The first step for segmenting the image was to apply global histogram thresholding by selecting an appropriate threshold value for the specific image. In practice, the assumption of bimodal histogram distribution is rarely the real case in US images, due to low contrast against the background. The median filtering adjusts the histogram for better discrimination between the grey level clusters, related to the target object and the background, respectively [3]. In global thresholding, any pixel value greater than the threshold T1 were set to 255 while pixel values smaller than T1 were set to 0. The procedure of global thresholding is illustrated by Eq(2):

$$g(x,y) = \begin{cases} 255 \text{ , if } f(x,y) > T_1 \\ 0 \text{ , if } f(x,y) \le T_1 \end{cases} \quad \text{Eq(2).}$$

A morphological 3x3 dilation filter was then applied to the binary image to fill the holes. In order to find the edges, the processed image was convolved with the Laplacian 3x3 mask to extract the edges of the target object . The mask is illustrated below:

Laplacian mask

0	-1	0
-1	4	-1
0	-1	0

The resulting image was in binary form, with black background and the target object identified with solid white color. An initial snake closed curve was specified manually, choosing preferably a number of 5 to 7 points around the target object. The intermediate pixels between the initial reference points were determined by piecewise linear interpolation functions. The initial polyline curve enclosed the target object.

The optimization process of adjusting this "snake" polyline, in order to fit exactly the edges of the target object, involved minimizing a combined set of energy-related functions. There are three basic types of energy associated with the snake [4]. These are: (i) the continuity term, which defines the elasticity of the snake, (ii) the rigidity, which describes the smoothness and avoids the oscillations of the snake by penalizing high contour curvatures, and (iii) the external energy factor, which describes characteristics of the image (intensity, gradient etc). The first two energy terms are described as "internal" and the third "external". The combined energy formula for the snake curve is depicted in Eq(8):

$$E_{snake} = \int_0^1 E_{\text{int}}\left[v(s)\right]ds + E_{ext}\left[v(s)\right]ds \quad \text{Eq (8)}$$

The E_{int} [v(s)] factor is the edge attraction term, defined in Eq(9):

$$E_{\text{int}}\left[v(s)\right] = 1/2\left[a(s)\left|\frac{\partial v(s)}{\partial s}\right| + \beta(s)\left|\frac{\partial^2 v(s)}{\partial s^2}\right|^2\right] \quad \text{Eq(9)}$$

The discrete equivalent of the formula is defined in Eq(10):

$$E_{\text{int}}[v(s)] = \sum_{N-1}^{i=0} a_i \left| v_i - v_{i-1}\right| + \sum_{i=0}^{N-1} \beta_i \left| v_{i-1} - 2v_i + v_{i+1}\right| \quad \text{Eq(10)}$$

The E_{int} [v(s)] factor is related to the minimization of distances between the snake's reference points, resulting in the curve "shrinking" closer around the target object. The first term of Eq(10) can also be described in the simpler form of Eq(11):

$$E_{cont} = \left(x_i - x_{i-1}\right)^2 + \left(y_i - y_{i-1}\right)^2 \quad \text{Eq(11).}$$

The second term of Eq(10) describes the second derivative of the initial polyline of the target object's boundaries and its curvature can be approximated by the finite difference formula of Eq(12):

$$E_{curv} = \left(x_i^2 - 2x_i + x_{i+1}\right)^2 + \left(y_i^2 - 2y_i + y_{i+1}\right)^2 \quad \text{Eq(12).}$$

The edge attraction term of Eq(9)-Eq(10) essentially shrinks the snake curve closer to the object's boundaries. In order to stop the shrinking process at the optimal positioning, an additional energy factor was essential for detecting the exact edges of the underlying object and relating it with the current position of the snake curve. This energy term was defined as the combination of gradients in Eq(13):

$$E_{ext} = -\left\|\nabla I\right\|^2 \quad \text{Eq(13).}$$

The snake optimization algorithm processed pairs of subsequent reference points, with relation to a 3x3 connectivity mask. The continuity and rigidity energy terms were calculated separetely and added together, subsequently subtracting the external energy term, in relation to the next reference point. The resulting 3x3 matrix contained the combined energies for each of the 8 neighbors of the current reference point. The direction in which this reference point should be moved can then be identified as the neighbor that pointed to a lower energy level. The same procedure was repeated for each reference point and the new reference positions were applied for the next iteration. When the snake reached the edges of the target object, the external energy term produced a large negative effect, thus "sinking" the

combined energy function into a low energy level [5]. As the reference points moved further into the inside area of the object, the energy level started rising again, producing a subsequent moving momentum towards the opposite direction. In essense, the reference points were trapped inside a sharp "valley" on the energy surface, related to the exact edges of the target object. The algorithm could then stop when no further minimization was possible, i.e. when no further moving was possible for the reference points. The next procedure included the usage of C++ routines to isolate the snake outline from the image and measure the surface in pixels.

Figure 2 : The ROI selected by the physician.

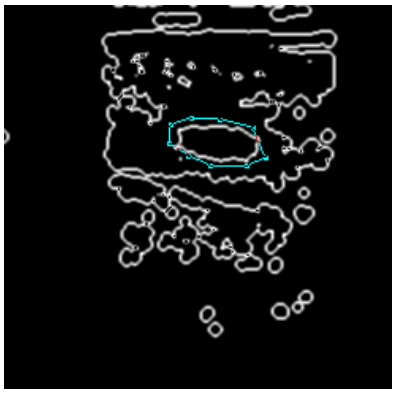

Figure 3: The initial Snake contour outlines the target contour produced by the edge detection algorithm.

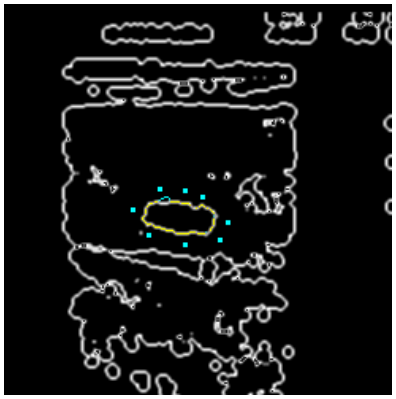

Figure 4: The Snakes is attracted by the edges and falls into the pit.

Figure 5: The shape of the object filled.

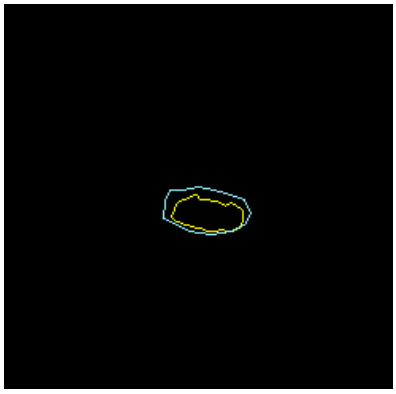

Figure 6: An overview of the difference between the manually and automatically outlined ROI, using no pre-processing algorithms.

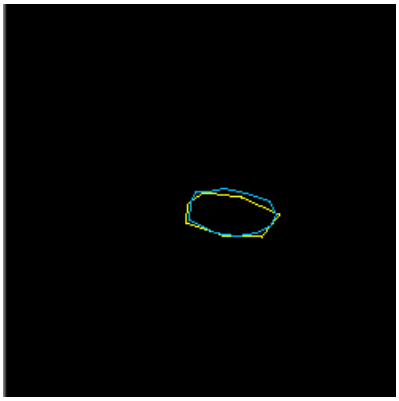

Figure 7: An overview of the difference between the manually and automatically outlined ROI, using HE and soft thresholding pre-processing algorithms.

3. Results

Images were processed by the proposed software and were compared with the physician's ROIs. The free-handed ROI selection by the physician, formed as a polygon, included an average number 12 to 15 points per image ROI. To investigate the impact of wavelet based pre-processing on boundary detection, three different pre-processing algorithms were tested. The first involved histogram equalization alone. The second included the 3-level wavelet soft-thresholding. The third comprised a pre-processing algorithm that combined both histogram equalization and soft-

thresholding. Surface differences between the physician's manually drawn ROIs and the automatically detected ones are shown in Table 1:

Table 1: Mean area differences between physician's manually drawn ROIs and corresponding automatically detected ROIs.

Preprocessing Algorithm	**Average Surface Difference (%)**
No Preprocessing	16.12
Histogram equalization (HE)	18.16
Soft Thresholding	9.71
HE+Soft Thresholding	8.56

4. Discussion

The average differences between hand-drawn and automatically detected ROIs without pre-processing was high due to the presence of image speckle noise, which caused discontinuities in the detected edges. The application of HE pre-processing, enhanced image contrast but also increased the presence of noise, resulting in increased surface differences between hand-drawn and automatically detected ROIs, as shown in Table 1. When soft thresholding was applied alone the average surface difference was reduced to 9.71%, most probably due to the despeckling effect of the algorithm. Average surface difference was further diminished to 8.56% when HE and soft-thresholding were combined. The drawback of the proposed method is in the proper selection of the parameters, such as the threshold of the wavelet shrinkage, the threshold of the histogram, and the user's subjective selection of initial snake points. Regarding processing time the proposed algorithm required approximately 2 to 3 seconds for a 256x256 image on a typical PC (Intel P4 1.9MHz).

5. Conclusion

The difficult task of automatically delineating ROIs on US mammograms may be assisted by proper combination of wavelet based preprocessing techniques and the efficient active contour algorithm.

6. References

[1] W. K. PRATT (1991): '*Digital Image Processing*' (Second Edition), John Wiley & Sons, New York, pp. 275-285.

[2] DONOHO D.L. (1995): 'DE-NOISING IEEE TRANS. INFORM. THEORY, VOL. 41, NO.3, PP. 613–627.

[3] R. C. GONZALES, R. E. WOODS (1992): '*Digital Image Processing*', Addison-Wesley, pp. 167- 1.

[4] N.E. DAVISON, H. EVIATAR , R.L. SOMORJAI: 'Snakes Simplified' accepted on 21 June 1999 Published by Elsevier Science Ltd on behalf of Pattern Recognition Society.

[5] TONY F. CHAN, *Member, IEEE,* and LUMINITY A. VESE : *IEEE TRANSACTIONS ON IMAGE PROCESSING, VOL. 10, NO. 2, FEBRUARY 2001*. 'Active Contours Without Edges'.